# A Digital Signal Amplification Device for Microelectrode Arrays based on Stochastic Resonance

Francisco FAMBRINI[1], João Batista DESTRO-FILHO[2], Luis Mariano Del Val CURA[3], Diego SAQUI[1,4], José Hiroki SAITO[1,3]
[1]*Computation Department, UFSCar – Federal University of São Carlos, São Carlos, Brazil*
[2]*UFU – Federal University of Uberlândia, Uberlândia, Brazil*
[3]*UNIFACCAMP – University Center of Campo Limpo Paulista, Campo Limpo Paulista, Brazil*
[4]*IFSULDEMINAS – Federal Institute of Sul of Minas Gerais, Muzambinho, Brazil*
*djhs@ufscar.br*

**Abstract—In this work, an experimental study was carried out about the construction of an amplification equipment based on the phenomenon of stochastic resonance (SR), which was initially thought to detect spikes and bursts from human and animal neuronal tissue, both in vitro (from microelectrode array, MEA) and in vivo, from electrodes in the cerebral cortex of mammals. The implemented equipment was called CADSR (Computer-Aided Digital Stochastic Resonator) and brings as innovation the fact of being controlled and monitored by the computer, through a graphical interface that allows an automatic tuning, making it possible to obtain the optimum level of noise to maintain SR in real-time. Experimental results show that for electrical signals from multi-electrode arrays with amplitude below 25 microvolts, the amplification system using stochastic resonance is better than conventional amplifier systems, which use operational amplifiers in linear configurations.**

***Index Terms*—multielectrode, signal, stochastic, resonance, amplifier.**

## I. INTRODUCTION

A planar Microelectrode Array (MEA) of *in-vitro* neuron culture is used to record extracellular electrophysiological signals, with the possibility of chemical or electrical stimulation before or during the signal recording. Basically, the device is composed of a culture chamber, similar to a Petri dish, where the biological cell culture is placed on a number of microelectrodes. MEA is used to record signals from neuronal tissue slices or dissociated neuron cultures, allowing the investigation of electrical spontaneous or stimulated activities of neurons, with or without the use of drugs or medicines. Fig. 1(A) shows a MEA60 device from Multichannel Systems [1] used in this work, and in Fig. 1(B), its microelectrodes in the center are highlighted.

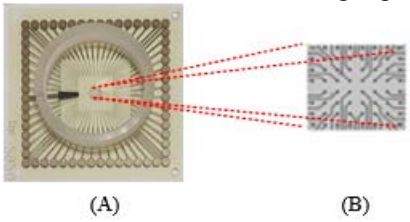


Figure 1. (A) MEA60 . (B) Amplified details of microelectrodes in the center of MEA60 multielectrode array

In this work experiments about the construction of MEA signal amplification equipment are realized based on the phenomenon of stochastic resonance (SR). Noise is generally detrimental to electronic systems because it limits performance, and great efforts are being made by physicists and engineers to reduce noise, such as filtering, feedback compensation, electromagnetic shielding, phase input, etc. However, in the last 40 years, several studies have demonstrated that many physical and biological systems work better in the presence of noise, such as biological neurons and electronic systems. Stochastic resonance is a term used to describe any phenomenon in which the presence of noise or noise applied on a nonlinear system improves the response to a particular input signal. This is a subject little known even by researchers in the area of Signal Processing. The SR occurs only in systems whose output presents non-linearity in relation to the applied input signal. An example of SR application is on static, dynamic, and functional balance in the elderly and in patients with neurodegenerative diseases [2]. A review of the applications of SR in rotating machine fault detection was described by Lu, He, and Wang [3]. A review of the impact of galvanic vestibular stimulation-induced SR on the output of the vestibular system was provided by Stefani, and Serrador [4]. Another interesting example of the application of the SR phenomenon in an electronic device was presented in the excellent article by Chiga, Tanaka, Yamazato, Tadokoro and Arai [5]. In this paper, the authors constructed a receiver for very weak signals of RF (Radio Frequency) based on Schmitt trigger electronic circuit, exemplifying the use of SR in wireless receiver systems [5]. Jayram and Mekuria described SR interference managing ontological cognitive radio for TV white space [6]. Another interesting paper is about a variant of SR termed Ghost Stochastic Resonance [7]. Some of the authors of this paper described in 2015 a very simple prototype of MEA signal amplification using SR, with only one channel, of an electronic circuit, generating white Gaussian noise, with amplitude adjusted manually [8], and in 2017, construction of a conventional system [9] of amplification of microelectrode signals, based on linear amplifiers, without the use of SR concept. In this paper it is presented an evolution of the first prototype described in [8], with the automatic detection of the

Digital Object Identifier 10.4316/AECE.2020.03004

resonance point using control software in a closed-loop, in a device denoted CADSR, based on the microcontroller ARM Cortex M4, with internal AD conversion, that digitalizes the signal and the noise, and measures their amplitudes automatically, adjusting the noise level to obtain the best signal-to-noise ratio, in each measured channel. The results of the amplification of the CADSR system and the conventional system [9] are compared in this paper.

Fig. 2(A) shows the model of a threshold-based Stochastic Resonance system [10]. The input signal to be measured is represented as the function $s(t)$, and $\eta(t)$ is the white Gaussian noise added to the input signal, resulting in the variable $x(t)$. The output of the system is represented by $y(t)$ which is equal to $T[x(t)]$ where $T[.]$ is a nonlinear transformation, that for a value of *x(t)* equal or above *T*, the result is different from zero, and zero otherwise. In this way, if the input *s(t)* is too small, the noise *η(t)* can be conveniently added to *x(t)* so that its value becomes equal or above *T*, and the output detects the input signal *s(t)*. A possible form for y(t)= $T[x(t)]$ is given in eq. (1):

$$y(t)\begin{cases}\neq 0 & if\ x(t)\geq T\\ =0 & if\ x(t)<T\end{cases} \quad (1)$$

where $T$ is a threshold determined experimentally. The Schmitt trigger (ST) is an electronic circuit capable of producing the SR phenomenon and is very simple to implement in practice from an operational amplifier (OA) voltage comparator, Fig. 2(B).

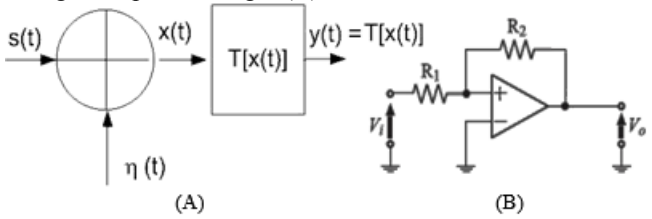


Figure 2. (A) Model of a SR system based on threshold; (B) Schmitt trigger circuit, assembled from OA

In Section II it is described the Brownian motion and Langevin equation, which provide a simple mathematical model capable of explaining the SR phenomenon in a simple particle example. In Section III, the Langevin equation is analyzed and numerically solved using Matlab software. Since it is proposed to investigate the use of SR in this work, in Section IV, are listed several methods to measure SR performance, and in Section V it is explained in detail the concept of signal-to-noise ratio (SNR), which is then used in this work. In Section VI, three nonlinear electronic circuits used to obtain SR are simulated, and one of them, that does not invert the input signal is chosen for the implementation. Then, as described in Section VII, the device called CADSR and its graphical interface were developed. In Section VIII two experiments are reported: E1) determining the resonance noise level of CADSR, and E2) comparing the performance between a conventional linear amplifier and the SR-based system. Finally, in Section IX it is presented the conclusions and future works.

## II. Brownian Motion and the Langevin Equation

The random motion of a particle (with a diameter around $10^{-3}\,mm$ immersed in a fluid with a density approximately equal to the particle is called Brownian motion [11]. Initial investigations of this phenomenon were made by biologist Robert Brown on pollen grains and also dust particles or other objects of colloidal size. Albert Einstein provided a first explanation for the Brownian motion in his Ph.D. Thesis, in 1905. He obtained a relation between the macroscopic diffusion constant D and the atomic properties of matter. The Brownian motion theory has been extended to situations in which the floating object is not a real particle but some collective property of a macroscopic system, for example, the instant concentration of any component of a chemically reactive system near thermal equilibrium. Here the irregular fluctuation in the time of this concentration corresponds to the irregular movement of the dust particle. Stochastic systems are found in different areas of physics: from the microscopic level, as verified in the diffusion of particles in a solvent, to astronomical order, as observed in stellar systems [12]. An interesting example of this latter type is represented by a black hole (BH) at the center of a dense star system. Theoretically, when the mass of the black hole is very large, it can acquire a movement that is similar to that of a suspended particle in a liquid or a gas [11]. In cosmology, Brownian motions are also used to study galaxies, galaxy clusters, and voids [13]. A non-linear bistable system is one of the typical SR models. Its essence is a Brownian particle overloaded in a bistable potential well, accompanied by the periodic motive force and noise [14]. The system can be modeled using the Langevin equation of motion in the form of the stochastic differential eq. (2):

$$\frac{dX(t)}{dt} = aX(t) - bX^3(t) + A\cos(\omega.t) + \eta(t) \quad (2)$$

$a>0$ and $b>0$ are system parameters, $X(t)$ is the output of the system (in the case of a particle, it is the position of the particle - remembering that $X(t)$ can be a vector with degree 3 of freedom and thus indicate the position of a particle in three-dimensional space, but here we will deal only with the one-dimensional case) and $A\cos(\omega.t)$ is the input signal. $A$ and $\omega$ are the amplitude and frequency of the input signal respectively. In addition, there is an additive noise with intensity $\eta(t)$. For the particular and simplified case where $A=0$ and $\eta(t)=0$, the non-linear bistable system takes the form of the summed eq. (3):

$$\frac{dX(t)}{dt} = aX(t) - bX^3(t). \quad (3)$$

For this simple case, the equation of the potential energy $U(t)$ acting on the particle whose position is $X(t)$ can be obtained by integration. This equation is given by (4), which is the classical equation of the simple symmetric bistable potential well, a biquadratic (fourth-order) equation in the variable $X$ :

$$U(X) = -\frac{a}{2}X^2 + \frac{b}{4}X^4. \quad (4)$$

The graph of the potential energy of the particle under Brownian motion, in the absence of additive noise and in the absence of external forces is then shown in Fig. 3.

From the graph shown in Fig. 3, it can be seen that there are two positions $X(t)$ where the particle is at the minimum

potential energy level: $X(t) = X_1 = -\sqrt{a/b}$ and $X(t) = X_2 = +\sqrt{a/b}$. In these two positions, although there is potential energy and both have the same energy level, the particle cannot theoretically exchange its position between them. The potential barrier separating the two points of coordinates $X_1$ and $X_2$ is equal to $\Delta U = a^2/4b$.

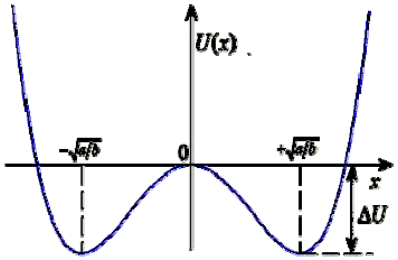


Figure 3. Graph showing the potential energy of a particle in Brownian motion, in the absence of additive noise and external forces

In a liquid where Brownian motion occurs, for example, it is the additive noise coming from the thermal agitation of the liquid molecules, the one responsible for moving the particle from position $X_1$ to position $X_2$. If a weak periodic force is applied to the particle, the double potential barrier is asymmetrically moved up and down, periodically increasing and decreasing potential. When synergy occurs between the signal and the noise, the energy of the particle becomes greater, than the potential barrier, and then the Stochastic Resonance occurs and the particle can move from the equilibrium point $X_1$ to $X_2$ and vice-versa. Due to the cooperation between signal and noise, there is the ideal noise intensity that can maximize the output response at frequency *f*. By increasing the noise intensity, many transitions are triggered by noise during a periodic input cycle, and the signal-to-noise cooperation is lost again. This is the SR effect: the system response is more regular at a finite and non-invasive noise level. There is no violation of the Laws of Thermodynamics here: the potential energy of particle before and after, the potential barrier transposition is absolutely the same. This model illustrates the operation of SR for a single particle immersed in a liquid [15].

## III. Numerical Analysis of The Langevin Equation

The Langevin equation (2) is a special type of differential equation, called stochastic because it presents a noise term. To solve this equation, the Runge-Kutta fourth-order algorithm was used in several software packages. In this work the software Matlab version R2014 was used. Eq. (2) was discretized to obtain a numerical solution and assumed the discrete form of eq. (5):

$$\Delta X = (aX - X^3)\Delta t + \beta \Delta \eta(t) \qquad (5)$$

where $\beta$ represents the amplitude of the noise summed with the momentary amplitude of the excitatory force $Fe(t) = A\cos(\omega, t)$ and $\Delta t$ represents discretized time intervals required for computer numerical simulation. Solving the discrete Langevin equation through Matlab software for $t_{max}$ =100, $\Delta t$ =0.01, $x_0 = 0$, $\alpha = 2$ and $\beta = 1$, the graph shown in Fig. 4 was obtained. Several graphs of the solutions for different values of $\alpha$, $\beta$ were plotted so that, for some values, particle oscillates for some time around one of the minimum values of the potential energy $U(x)$ and eventually transits to the other minimum. For other values of the parameters, the particle does not pass between the minimums. The Stochastic Resonance occurs when the transition period between the minima equals the period of the excitatory $Fe(t)$ Force and for this reason, it allows us to detect this force more easily. For the simulations shown in Fig. 4, $\Delta t$ =0.01, the maximum time was made equal to $t_{max}$ =100 and the initial position of the particle is $x(0)$ =1 in all cases. Note in Fig. 4(A) that the minimum energy points correspond to the ordinates $P_1 = -1.5$ and $P_2 = +1.5$. The particle oscillates between these two equilibrium points and the energy for the oscillation comes from the sum of the excitatory force $Fe(t)$ and the noise is responsible for the stochastic resonance process. Fig. 4(B) shows the Amplitude Spectrum obtained from the Fast Fourier Transform (FFT) for the same graph obtained in Fig. 4(A). A peak can be observed in the oscillation frequency of the excitatory force $Fe(t)$, i.e. 0.1 Hz.

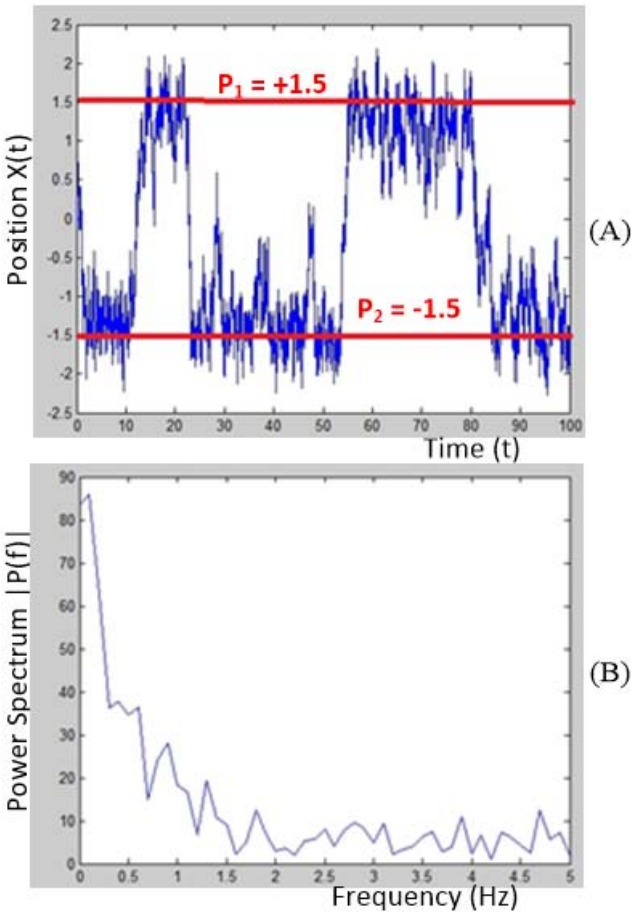


Figure 4. (A) Solution of the equation of trajectory (5) for a particle in Brownian motion performing Stochastic Resonance with the additive noise. In this simulation the values of the chosen parameters were: $\alpha = 2$, $\beta = 1$, $t_{max}$ =100, $\Delta t$ = 0.01 and $x_0 = 0$; (B) FFT for the signal shown in (A)

It can be seen that in Fig. 5(A), for $\alpha = 2$ and $\beta = 1$, the particle oscillates between two equilibrium points, which correspond to the minimum energy points of the double potential well; these points are marked by the green lines. In this case, the frequency of the excitatory force $Fe(t)$ whose

frequency is 0.1 Hz (corresponding to the weak signal to be detected through SR) is visualized in the lower graph by a peak in the power spectrum graph, shown in green arrow. In Fig. 5(B) for $\alpha = 0.5$ and $\beta = 2$ it is not possible to identify two points around which the particle oscillates and this can be confirmed by the absence of significant peaks of the lower (B) graph , which shows the frequency domain. In Fig. 5(C) , for $\alpha$ = 5 and $\beta$ =0.5, the particle seems to oscillate around a single point of coordinate $X = 2.25$ with the frequency of 0.1Hz which is the frequency of the excitatory force (which can be confirmed by the lower graph). Finally, in Fig. 5(D) for $\alpha = 0.5$ and $\beta = 5$ , the particle does not appear to oscillate between two distinct points, which can be noticed by the absence of much larger peaks in (D) lower graph.

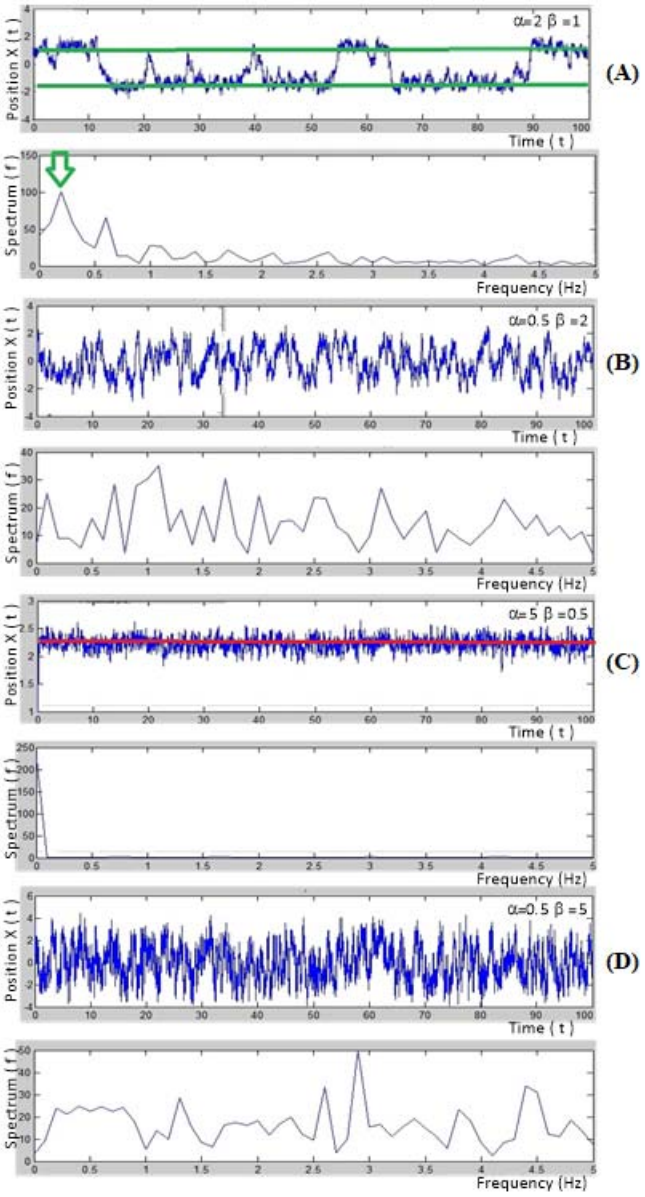


Figure 5. Results of solution of discrete Langevin equation (5) for different values of the parameters α and β. (A) $\alpha = 2$ and $\beta = 1$ ; (B ) $\alpha = 0.5$ and $\beta = 2$ ; (C) $\alpha = 5$ and $\beta = 0.5$ ; (D) $\alpha = 0.5$ and $\beta = 5$ ; On the lower side, are shown the frequency spectra of each signal using FFT calculations

The lower graph in Fig. 5(D) seems to show a much more uniform distribution of noise amplitude, evidencing several frequencies, which characterizes the predominance of white noise. Similar behaviour occurs with Fig. 5(B) lower graph.

## IV. Performance Measures for SR

By the fact that we are proposing an innovative digital signal amplification device using SR, this section describes the performance measures for SR to amplify signals in general, and the next section describes the chosen method in detail. The performance of Stochastic Resonance to amplify signal and information has been measured in several different ways, as described in the literature. As measurement techniques for the improvement obtained for the signal, it is mentioned: a) Signal-to-noise ratio measurements - SNR [16]; b) Amplification of spectral power [17-22]; c) Correlation coefficient [23]; d) Mutual information [24]; e) Kullback's entropy [25]; f) Channel capacity [26-27]; h) Differences - φ [28]; and i) Mean square distortion [29].

Stochastic Resonance was also analyzed in terms of time distributions [30], as well as the Receiver Operating Characteristic (ROC) method [20-21], which are based on probabilities of detecting a signal to be present, or falsely detecting a non-existent signal [27]. In this work, it was chosen to measure the performance of SR amplifying device using the SNR method, because it is the most appropriate considering the available instrumentation by the authors, that makes use of Fast Fourier Transform (FFT), and also because it is a method well described in the literature. The following section describes SNR, in detail.

## V. Signal to Noise Ratio (SNR)

The Signal to Noise Ratio (SNR) is the ratio between the power of the signal that transmits the information and the noise:

$$SNR = \frac{P_{signal}}{P_{noise}} \tag{6}$$

In equation (6), $P_{signal}$ represents the mean power of the signal and $P_{noise}$ represents the mean power of noise only, which must be measured at the same point in the circuit and under the same bandwidth. If the signal and noise are measured on the same impedance, then the SNR is given by the ratio of the amplitude of each of them, according to equation (7):

$$SNR = \frac{A_{signal}}{A_{noise}} = \left( \frac{\sqrt[2]{\frac{1}{n}\sum_{k=1}^{n} s_k^2}}{\sqrt[2]{\frac{1}{n}\sum_{k=1}^{n} r_k^2}} \right)^2 \tag{7}$$

where:

$A$ is the root mean square value (RMS) of the amplitude of signal or noise;

$s$ is the vector that represents the original signal;

$r$ represents the noise vector; and

$n$ is the length of the signal vector.

The SNR can also be measured in dB (decibels) through the relation given by eq. (8):

$$SNR_{db} = 10\log_{10}\left(\frac{P_{signal}}{P_{noise}}\right) = 20\log_{10}\left(\frac{A_{signal}}{A_{noise}}\right) \tag{8}$$

## VI. Simulation of Nonlinear Amplifier Circuits

To implement the bistable nonlinear circuit required to obtain the SR phenomenon by mixing a very weak signal with noise, three circuits were simulated and analyzed from the standpoint of introducing non-linearity into the signal applied at its input. The first circuit, Fig. 6(A), is a classic Schmitt trigger described in the literature, based on a single operational amplifier; the second circuit is a nonlinear amplifier with an "*N*" shape curve Fig. 6(B), described by G.P.Harmer, B.R.Davis, and D. Abbott [31] and the third circuit is a nonlinear amplifier with an "*S*" shape curve Fig. 6 (C), described by M.S. Adeel and U. Rashid [32].

From the results of the simulations, a prototype was constructed and the circuit chosen was that of Fig. 6(C) due to not inversion of the input signal phase.

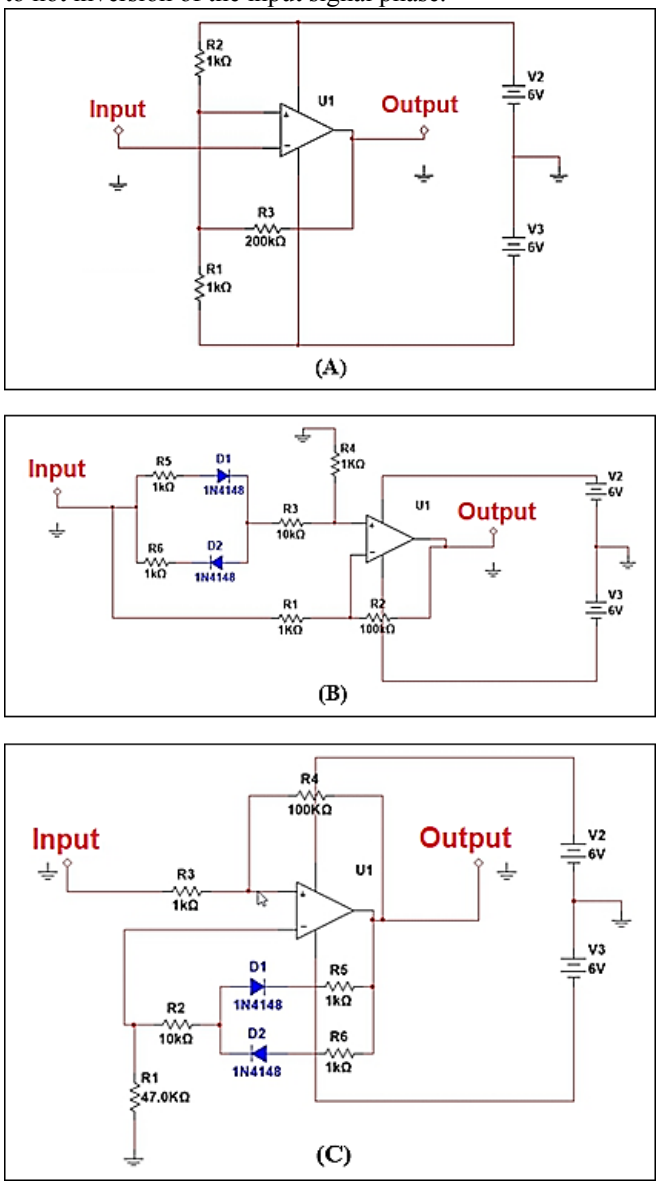


Figure 6. (A) Schimitt trigger classic; (B) "N-shape" transfer function non-linear amplifier; (C) "S-shape" transfer function non-linear amplifier

In Fig. 7, the simulation of the three circuits is illustrated. In each screen, a pair of signals (input–output) of the respective circuit is shown: (A-B) Conventional Schmitt trigger; (C-D) Non-linear amplifier with phase inversion; and (E-F) Non-linear amplifier without phase inversion. These images were obtained from Multisim SPICE Simulator software, provided by National Instruments. It can be seen that the first two pairs (A-B), and (C–D) are inverted, differently from the last pair (E–F).

## VII. CADSR (Computer-Aided Digital Stochastic Resonator)

The circuit of Fig. 6(C) was implemented as part of a larger device called CADSR (Computer-Aided Digital Stochastic Resonator) whose block diagram is shown in Fig.8. The electronic circuits used in CADSR are classical circuits. The innovative idea presented in this work is the use of the classic circuits to introduce SR concepts, and the SNR measurement in real-time, using a fast microcontroller (ARM Cortex M4), searching automatically the SR point through computer, with the graphical interface of CADSR.

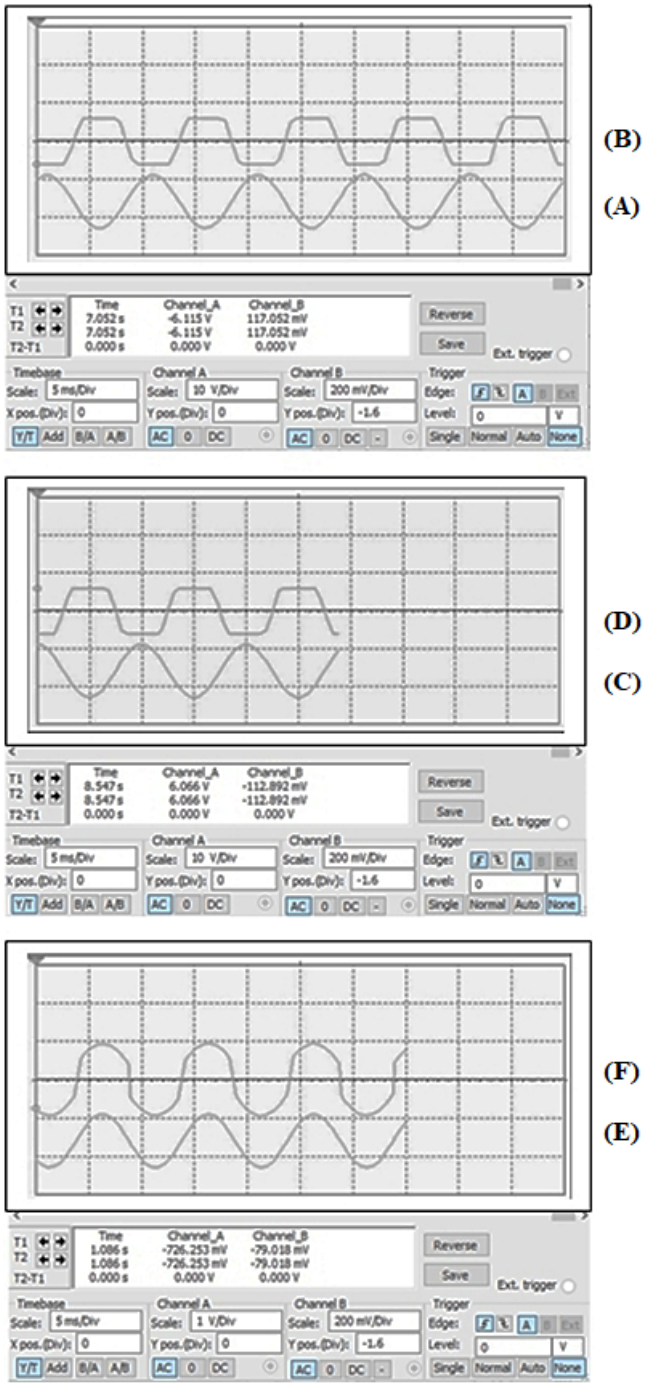


Figure 7. Simulation Results (input – output): (A-B) Conventional Schmitt trigger circuit; (C-D) Non-linear amplifier with phase inversion; and (E-F) Non-linear amplifier without phase inversion

Each of the circuits shown in block in the diagram of Fig. 8 was simulated separately and individually mounted on a specific printed circuit board. The microcontroller-ADC system used as a block (11) performs readings with a sample rate equals 10,000 samples per second, and theoretically, according to the Nyquist limit, it can sample frequency signals up to 5 kHz. For the electronic control of the amplitude levels of the electrical signals, digital potentiometers (showed in blocks (1) to (4)), model X9313 provided by Renesas Co. [33] were used. Each digital potentiometer can be adjusted in 32 different levels, with values ranging from 0 to 31.

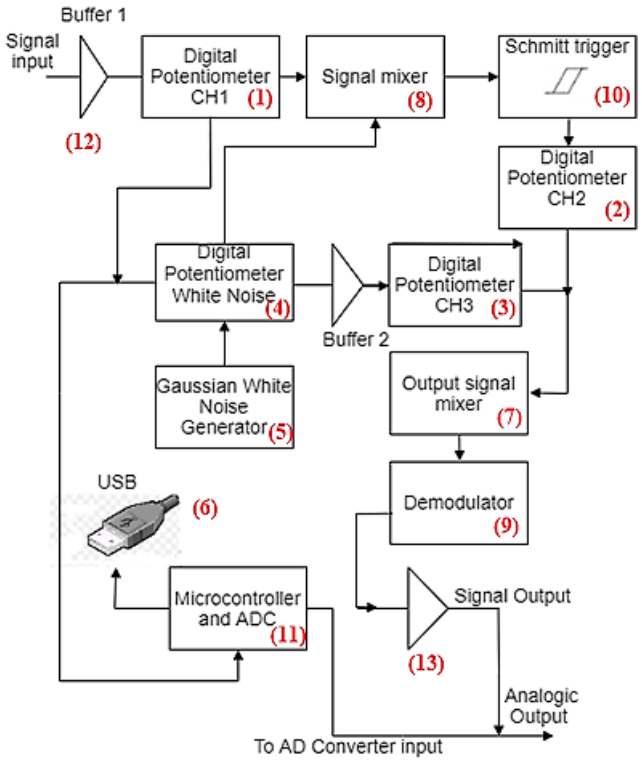


Figure 8. Block diagram of the electronic system composing the CADSR device

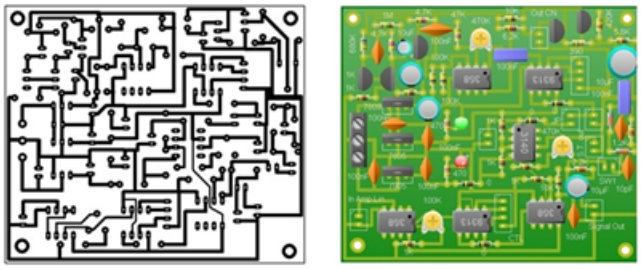


Figure 9. Printed circuit board of CADSR analog electronic system

The Gaussian white noise generator, block (5), is based in reverse polarized diode junction. The block (6) is an USB connector to computer. The signal mixers, blocks (7) and (8), are responsible to mix white noise and signal input. Optional demodulator, block (9), when activated, can extract changes in signal amplitude at the output. The Schmitt trigger, block (10), corresponds to circuit showed in Fig. 6(C), the best choice for this application. Finally, the output signal is applied at microcontroller-ADC system input. Blocks (12 and 13) are buffers of operational amplifier isolator stages.

In Fig. 9 it is showed the printed circuit board of CADSR analogic parts, without the microcontroller-ADC system, which is coupled outside.

To control the CADSR equipment through computer software it was developed a graphical interface, Fig. 10, that shows the Gaussian noise generated by the device itself added to the RMS value of the signal, present at the output of the equipment, plots in (A), and also calculates and shows in real-time the SNR values in (C) and SNR (dB) in (F). On the right side of the interface, marked with (D) there are four windows that allow us to adjust the values of the following constants: KWN (White Noise constant), KCH1, KCH2 and KCH3. These constants adjust the scaling factor of each potentiometer so that the value shown on the screen of the graphic interface coincides with the RMS voltage value generated at the output of each stage. These four constants have their values adjusted by the oscilloscope using the following procedure: 1- The RMS value of the white noise generated when the potentiometer is placed at level 16 (middle of the scale) is measured; this value (given in millivolts) is divided by 16 to produce the correct value of the constant KWN; the constant KWN is then set to this value;

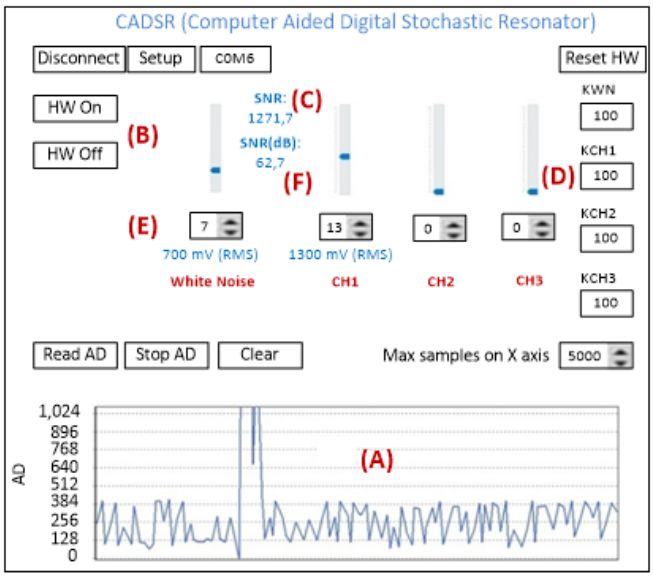


Figure 10. Aspect of the graphic interface of CADSR Device Control Software

2- The potentiometer is then varied and the value showed in (E) is checked with the value of the RMS voltage amplitude shown by a digital oscilloscope. The same procedure is also repeated for the other three potentiometers CH1, CH2, and CH3, by measuring their RMS values with the oscilloscope in the electronic circuit. A closed-loop routine optionally allows the noise amplitude to be automatically varied by means of the computer, so as to always obtain the highest SNR value, creating a device capable of stochastic auto-tuning. This "SR auto-tuning function" can be turned on pressing the button (B).

The experimental setup for measurement is shown in Fig. 11: (1) MEA socket with linear amplifiers inside it; (2) Temperature controller, in order to heat the biological culture at 37 degrees Celsius; and (3) CADSR analog unit and microcontroller-ADC system.

## VIII. Experimental Results

Two experiments are reported in this section, for the evaluation of the performance of the experimental setup of Fig. 11: E1) determining the resonance noise level of CADSR, taking into account sinusoidal signals applied at the input, amplitude of the order of 50 μV, and E2) comparing the performance between a conventional linear amplifier and the SR-based system.

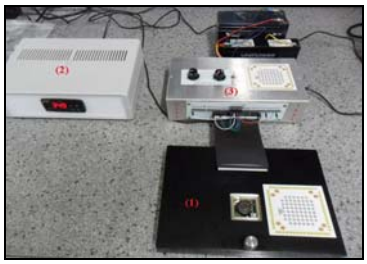

Figure 11. Experimental setup: (1) MEA Socket and linear amplifiers; (2) Temperature control; (3) CADSR System

Starting with the experiment E1, Fig. 12 and 13 shows the results obtained with CADSR amplifier, varying the input noise, from 2.5 mV to 10 mV; and from 15 mV to 40 mV, respectively. In several oscilloscope screen copies of both figures, two signals are shown: in blue, above, it is showed the signal presented at output CADSR system and below, in yellow lines, the level of Gaussian white noise, used in order to obtain Stochastic Resonance amplification. Table I shows the respective values of the input noise intensity (mV), detected output signal level (mV pp), signal to noise ratio in dB, and total output gain in dB, for all tests performed in Fig. 12 and 13. It is important to note that the noise levels in these figures are amplified by a factor of 100, by a special amplifier build only for visualization, since in the Tektronix oscilloscope model TBS 1102B, used in the experiment, noise of 2.5 mV mingles with the instrument noise itself.

TABLE I. Results from Tests in Fig. 12 and Fig. 13

| Tests in Fig. 12 and 13 | Input noise (mV) | Signal+noise (mV pp) | SNR (dB) | Total output amplification gain (dB) |
|---|---|---|---|---|
| (A) - Fig. 12 | 2.5 | 9.95 | 12.0 | 46.0 |
| (B) - Fig. 12 | 5.0 | 315.00 | 36.0 | 76.0 |
| **(C) - Fig. 12** | **7.5** | **1334.00** | **45.0** | **88.6 (*)** |
| (D) - Fig. 12 | 10.0 | 1259.00 | 42.0 | 88.0 |
| (A) - Fig. 13 | 15.0 | 1191.00 | 38.0 | 87.4 |
| (B) - Fig. 13 | 20.0 | 796.00 | 32.0 | 84.0 |
| (C) - Fig. 13 | 30.0 | 559.00 | 25.4 | 81.0 |
| (D) - Fig. 13 | 40.0 | 400.00 | 20.0 | 78.0 |

The noise level and the signal was experimentally varied by digital potentiometer WN (white noise) and CH1 from the graphical interface of the CADSR, and adjusted to get the signals shown in Fig. 12 and 13. When the HW button in CADSR Computer interface is pressed on, the software looks for the best level of noise in order to obtain the SR effect in real-time, which is the "auto-tuning" function. It can be seen, from the graph of Fig. 14, that the point where SR occurs is where the amplitude of the noise is equal to 7.5 mV, highlighted as (*), which allows an RMS value for the output signal (sinusoid added to the noise) equal to 45 dB. In this situation, the overall gain of the system was recorded around 88 dB considering only the signal amplitude applied at the input.

The experiment E1 just described was to determine the optimum noise level of CADSR to explore signal amplification with the SR effect.

The experiment E2 will use noise level determined in the experiment E1 and verify the effectiveness of the CADSR amplifier equipment, compared with a conventional linear amplification system.

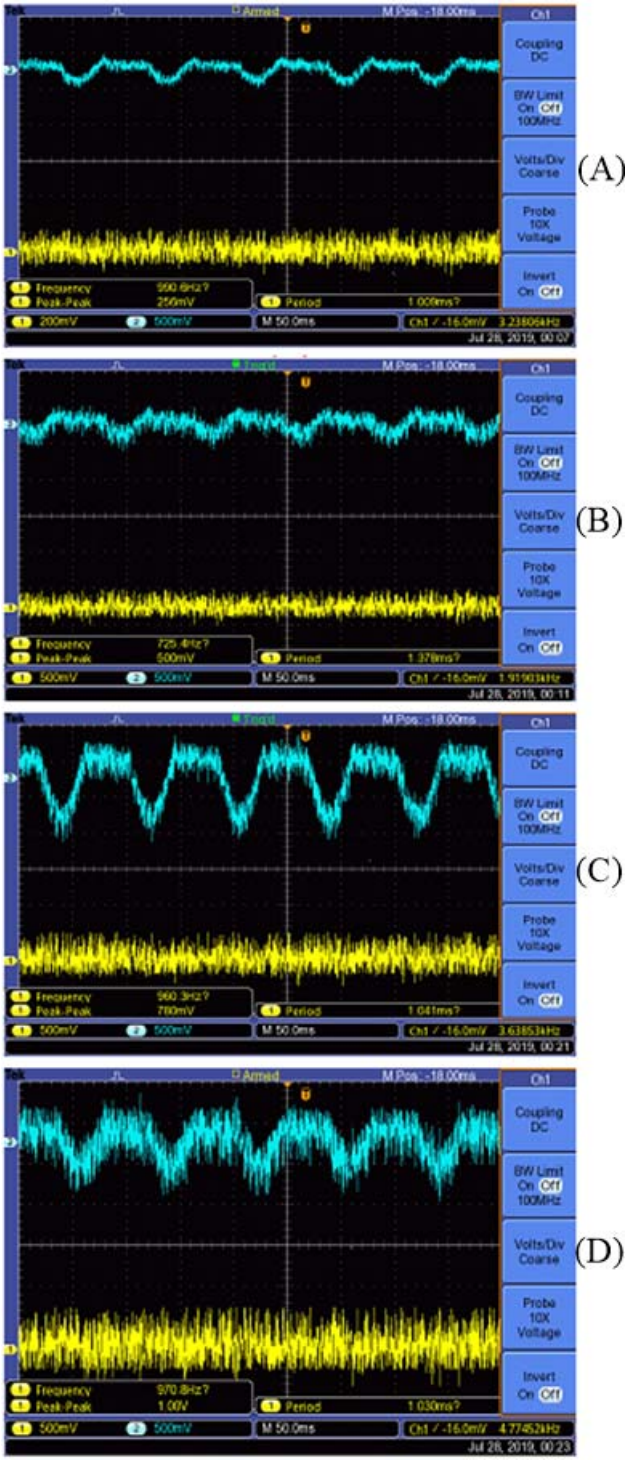


Figure 12. Oscilloscope screen of output signal, blue lines, of CADSR, varying the input noise, yellow lines: (A) input noise of 2.5 mV; (B) input noise of 5 mV; (C) input noise of 7.5 mV; and (D) input noise of 10 mV

Aiming this goal, it was programmed into a Minipa Function Generator, model MFG4210-B, a signal with frequency equal to 12 Hz, period 0.0833 s, containing 6 pulses, width of 600 μs in each period, followed by a "refractory" period where the wave remains at a low logical

level for another 0.0833s, as shown in Fig. 15. The signal was programmed in this waveform because it resembles the electrical impulses emitted by a neuron when it triggers a burst of pulses (set of spikes).

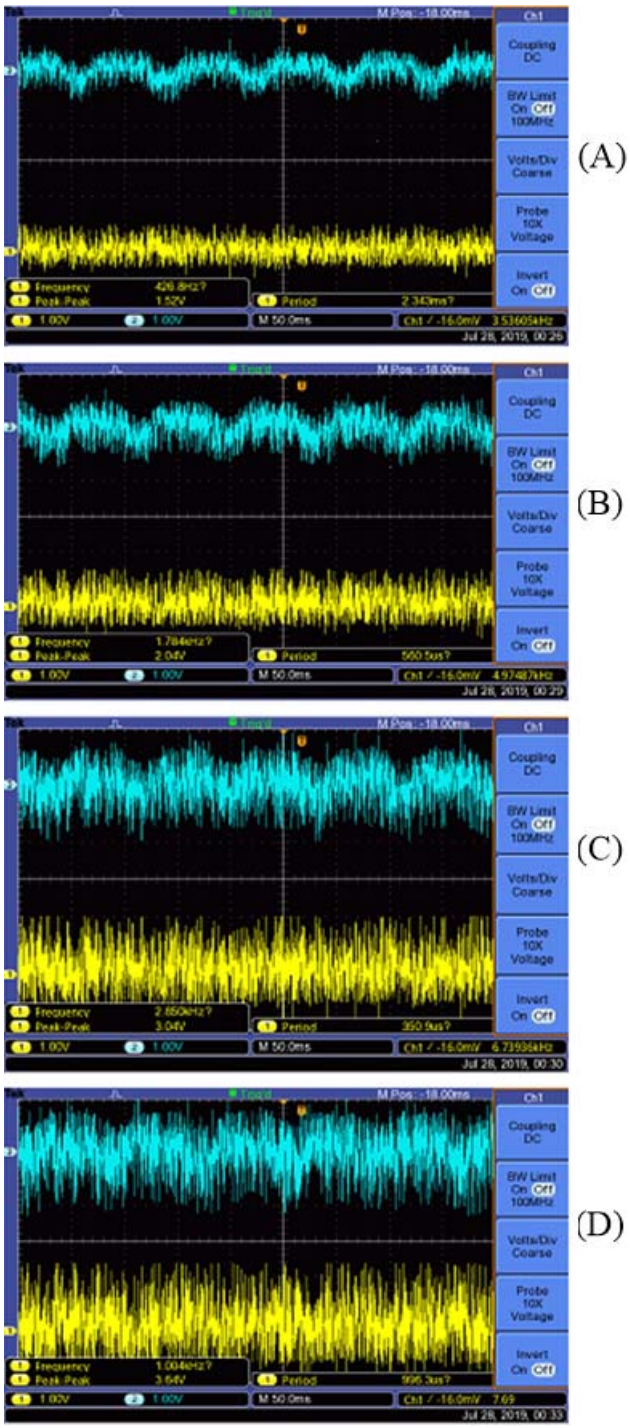


Figure 13. Oscilloscope screen of output amplified signal, blue lines, of CADSR, varying the input noise: (A) input noise of 15 mV; (B) input noise of 20mV; (C) input noise of 30 mV; and (D) input noise of 40 mV

The programmed signal was applied in tests in which the obtained outputs are shown in Fig. 16 (A-E), where: the upper yellow signal represents CADSR output and the blue lower signal represents linear amplifiers outputs. Table II shows the amplitude of the input signal and noise amplitude of both amplifiers. The Table III shows the results of the experiment with the proposed solution using stochastic resonance (CADSR output Level) compared against conventional amplifiers (Linear amplifier output). In the lowest two rows, of input level 25 and 10 Vpp, it can be verified that the linear amplifier could not detect the signal, differently from CADSR amplifier. The graph in Fig. 17 shows the gain in dB of two amplification systems (CADSR and conventional linear OA) in the same axis system.

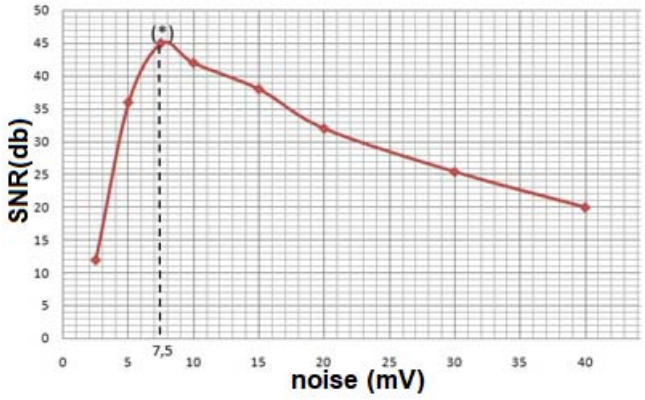


Figure 14. Graph showing SNR(dB) in CADSR output, against the noise level variation, highlighting the resonance noise level of 7.5 mV

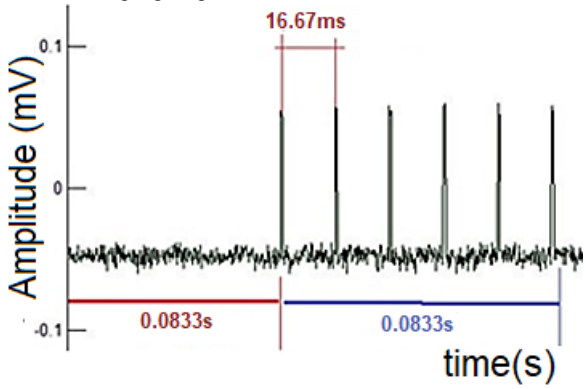


Figure 15. Graph showing the waveform programmed for comparative tests between the conventional amplification system and the CADSR stochastic resonance system

TABLE II. PARAMETERS ON GRAPHS OF FIG. 16

| Parameter | (A) | (B) | (C) | (D) | (E) |
|---|---|---|---|---|---|
| Input signal amplitude | 100 uV | 75 uV | 50 uV | 25 uV | 10 uV |
| Noise amplitude in conventional amplifier | 38 mV | 43 mV | 42mV | 43 mV | 54 mV |
| Noise amplitude in SR amplifier | 7.5 mV | 7.5 mV | 7.5 mV | 7.5 mV | 7.5 mV |

TABLE III. COMPARATIVE RESULTS BETWEEN CADSR AND LINEAR AMPLIFIER

| Input level (µV pp) | CADSR Output Level (mV p-p) | Linear amplifier Output Level (mV p-p) | CADSR voltage gain (dB) | Linear amplifier voltage gain (dB) |
|---|---|---|---|---|
| 100 | 276 | 158 | 68.8 | 63.8 |
| 75 | 268 | 82 | 71.0 | 60.8 |
| 50 | 268 | 62 | 74.6 | 61.8 |
| 25 | 264 | undetectable | 80.4 | --- |
| 10 | 264 | undetectable | 88.4 | --- |

## IX. CONCLUSION AND FUTURE WORK

It was developed a CADSR amplifier using the SR effect, for MEA signals, with a computational method for automatic search of Stochastic Resonance noise level, based on the measurement of the SNR in real-time by using microcontroller and computer.

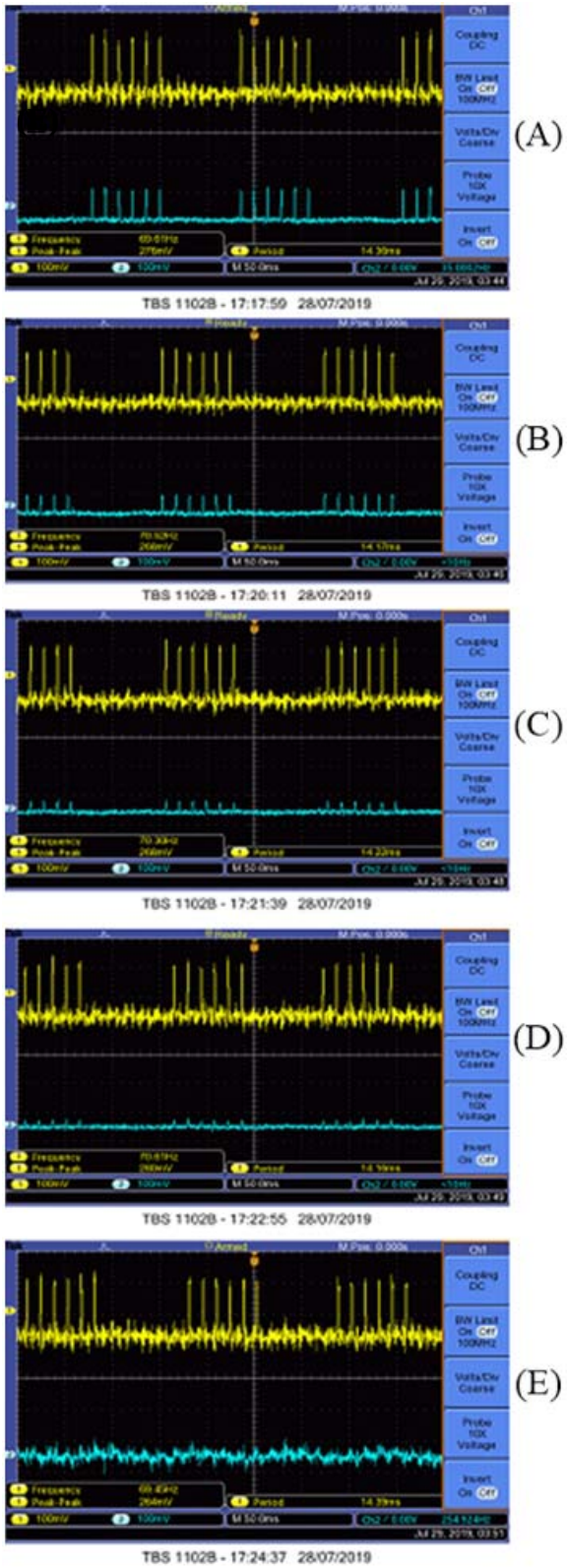


Figure 16. Print screen of the oscilloscope; with obtained data shown in Table III

Experiments were realized for determining the resonance noise level, and comparing CADSR with a conventional linear amplification system, applying in both systems, the same greatly attenuated input signal, and observed: a) For the conventional amplification system, the gain was always of the order of 62dB (1127 times, fixed by R-net in linear operational amplifiers), but when the input signal has amplitude below 25µV pp, it becomes undetectable, because the noise level is greater than the signal level present at its input; b) For the CADSR based system, the gain ranges from 68.8 dB to 88.4 dB. The gain increases as the input signal strength are attenuated due to the additive white noise beneficial action, producing SR effect, allowing very low signal detection; c) For signals with amplitude greater than 100µV p-p, the gains from both systems are virtually equal and there are no advantages in employing CADSR. This fact can be demonstrated by looking at the graph in Fig. 17.

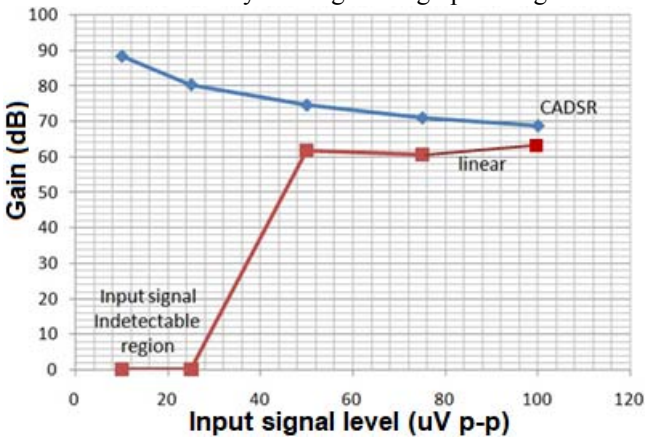


Figure 17. Comparison between the gains (dB) of the Stochastic Resonance amplification system (CADSR) (upper curve) and the conventional linear amplifier system (lower curve)

The SR amplification system, such as CADSR, is well suited for detecting spikes and bursts in signals produced by biological neurons, as in the MEA-based application. Even very low-intensity signals can be detected. In the conventional system, such signals are confused with the instrumentation noise level itself, and thus become undetectable. The optimal noise level of 7.5 mV that allowed the best signal detection through CADSR remained constant for input signals in the range of 10µV to 100µV p-p. The noise level was the same as that already measured in the test performed with the MEASim simulator (7.5 mV p-p) in sine wave [8]. Further investigation into this fact is needed because that is an unexpected result. By applying a sinusoidal wave to the input of both systems the conventional amplifier faithfully reproduces the wave, preserving its shape; the CADSR amplifier deforms the sinusoid, but its spectral components are still present and detectable by the Fourier Transform (FFT) applied to the resulting signal at the CADSR output.

Nature uses the SR phenomenon to propagate electrical impulses between neurons within the brain and also in the transmission of nerve impulses from sense organs, such as in the transmission of electrical signals from the retina and auditory nerves to the brain [35]. It seems natural to use the same SR effects to electronically amplify the signals from in vitro cultured neurons in MEA; in fact, the tests developed in this work were very promising for the adoption of this system when the main objective is to record spikes and bursts from in vitro neuronal activity. It is a fact that if it is desired to analyze the exact format of the electrical signal, the option of using the SR amplifier cannot be employed. However, for the purpose of this work (i.e., recording neuron signals in MEA) the SR-based system proved better than conventional linear amplifiers. Brain-Computer Interfaces (BCI) systems and electroencephalogram equipment (EEG) can also benefit from the SR method

when the most important is not to know the exact waveform produced, but to record the electrical impulses triggered by the activity of the neurons (spikes and bursts), which are often less than the intensity of instrumentation noise. Chopper amplifier is an alternative to amplify low signals, and to compare it with SR amplifiers deserves investigations. About SR, there are still several questions to be answered, including: a) How to determine analytically the optimal signal level for SR [34]? b) Is this noise signal level constant or does it vary with the signal amplitude present at the input system? c) Does the optimal signal enabling SR depend on the frequency of the signal to be detected? d) Is it possible to improve the performance of artificial neural networks with the controlled addition of noise? e) Can SR phenomenon be used to build more robust electroencephalogram recording equipment for use in the Hospital's Intensive Care Units?

## ACKNOWLEDGMENT

The authors acknowledge CAPES (Coordenação de Aperfeiçoamento de Pessoal de Ensino Superior), Ministry of Education, Brazil, Financing Code 001, and FAPESP (Fundação de Amparo à Pesquisa do Estado de São Paulo) by support of PIPE 2017/50270-5 Project.

## REFERENCES

[1] Multichannell Systems. Acessed on line in December 2019, https://www.multichannelsystems.com/products/microelectrode-arrays/60mea10010ir-ti

[2] S.Rogan, R.Hilfiker, A.Schenk, A.Vogler, and J.Taeymans, "Effects of Whole-body Vibration with Stochastic Resonance on Balance in Persons with Balance Disability and Falls History – A Systematic Review", Researchs in Sports Medicine, 22, 294-313, 2014. DOI: 10.1080/15438627.2014.919504

[3] S.Lu, Q.He, and J. Wang, "A review of stochastic resonance in rotating machine fault detection", Mechanical Systems and Signal Processing, 116, 230-260, 2019. DOI: 10.1016/j.ymssp2018.06.032

[4] S.P.Stefani, and J.M.Serrador, "Impact of galvanic vestibular stimulation-induced stochastic resonance on the output of the vestibular system: A systematic review", Brain Stimulation, 13, 533-535, 2020. DOI: 10.1016/j.brs.2020.01.006

[5] K.Chiga, H.Tanaka, T.Yamazato, Y.Tadokoro, and S. Arai. "Development of add-on stochastic resonance device for the detection of subthreshold RF signals", Nagoya University, Nolta, IEICE, 2015. DOI: 10.1588/nolta.6.520

[6] S.Jayram, K.Ouahada, F.Mekuria, "Stochastic Resonant Interference Managing Ontological Cognitive Radio for TV White Space", Proceedings of the International Conference on Advances in Computing and Communication Engineering (ICACCE), 28-29 Nov., pp. 336-341, 2016. DOI: 10.1109/ICACCE.2016.8073771

[7] P. Balenzuela, H.Braun, D.R.Chialvo, "The ghost of stochastic resonance: an introductory review", Contemporary Physics, 53, 1, 17-38, 2012. DOI: 10.1080/00107514.2011.639605

[8] M.A.Barreto, F. Fambrini, J. H. Saito, "Microelectrode array signal amplification using stochastic resonance". Industrial Electronics Society, IECON 2015 - 41st Annual Conference of the IEEE, pp: 2030 – 2035, Yokohama, Japan, 2015. DOI: 10.1109/IECON.2017.8217495

[9] F.Fambrini, J.H.Saito, L.M.D.V.Cura. MEA recording system circuit implementation. Industrial Electronics Society, IECON 2017 – 43th Annual Conference of the IEEE, pp: 8515-8520, Beijing. IECON 2017. DOI: 10.1109/IECON.2017.8217495

[10] M.D.McDonnell, N.G.Stocks, C. E. M. Pearce, D. Abbott, "Stochastic Resonance: From Suprathreshold Stochastic Resonance to Stochastic Signal Quantization". New York, Cambridge Un. Press, 2008. DOI: 10.1080/00107510903318814

[11] F. Jaramillo, K. Wiesenfeld, "Mechano electrical transduction assisted by Brownian motion: a role for noise in the auditory system", NatureNeuroscience, 1, 384–388, 1998. DOI: 10.1038/1597

[12] S. Chandrasekhar, "Stochastic Problems in Physics and Astronomy", Rev. Mod. Phys. 15, 1. 1943. DOI: 10.1103/RevModPhys.15.1

[13] P. Chatterjee, L.Hernquist, A. Loeb, Brownian Motion in Gravitationally Interacting Systems . Phys Rev.Lett. 88, 121103, 2002. DOI: 10.1103/PhysRevLett.88.121103

[14] S. Vitali, V. Sposini, O. Sliusarenko, P. Paradisi, G. Castellani, G. Pagnini, "Langevin equation in complex media and anomalous diffusion". J. R. Soc. Interface 15: 20180282, 2018. DOI: 10.1098/rsif.2018.0282.

[15] Y.Gao, L.Xiao, "Simulation of weak signal detection based on stochastic resonance". Proceedings of the Third International Symposium on Electronic Commerce and Security Workshops(ISECS '10) Guangzhou, P. R. China, 29-31, pp. 329-331, 2010.

[16] R. Benzi, G. Parisi, A. Sutera and A. Vulpiani, "Stochastic resonance in climatic change", Tellus 34:10, 1982.

[17] P. Hanggi, "Stochastic resonance in biology: how noise can enhance detection of weak signals and help improve biological information processing" , Chemphyschem, 3, 285–290, 2002. DOI: 10.1002/1439-7641(20020315)3:3<285::AID-CPHC285>3.0.CO;2-A

[18] P. Hanggi, M. E. Inchiosa, D. Fogliatti, A. R. Bulsara, "Nonlinear stochastic resonance: the saga of anomalous output-input gain", Physical Review E, 62, 6155–6163, 2000.

[19] P. Hanggi, P. Jung, C. Zerbe, F. Moss, "Can colored noise improve stochastic resonance, Journal of Statistical Physics", 70, 25–47, 1993. DOI: 10.1371/journal.pone.0091345

[20] R. Rozenfeld, L. Schimansky-Geier, "Array-enhanced stochastic resonance in finite systems", Chaos, Solitons and Fractals, 11, 1937–1944, 2000. DOI: 10.1016/S0960-0779(99)00133-2

[21] P. Imkeller, I. Pavlyukevich, "Stochastic resonance in two-state Markow chains" , Archiv der Mathematik, 77, 107–115, 2001. DOI: 10.1007/PL00000461

[22] K. Drozhdin,. "Stochastic resonance in ferroelectric TGS crystals" , PhD. thesis, Mathematisch-Naturwissenschaftlich-Technischen Fakult¨at der Martin-Luther-Universit¨at Halle-Wittenberg, 2001.

[23] J. J. Collins, C. C. Chow, T. T. Imhoff, "Aperiodic stochastic resonance inexcitable systems", Physical Review E, 52, R3321–R3324, 1995. DOI: 10.1103/PhysRevE.52.R3321

[24] J. E. Levin, J. P. Miller, "Broadband neural encoding in the cricket cercal sensory system enhanced by stochastic resonance", Nature, 380, 165–168, 1996. DOI: 10.1038/380165a0

[25] A. Neiman, A. Silchenko, V. Anishchenko, L. Schimansky-Geier, "Stochastic resonance: noise-enhanced phase coherence", Physical Review E, 58,7118–7125. Part A, 1998. DOI: 10.1007/978-3-0348-8287-3_14

[26] D. Rousseau, F. Chapeau-Blondeau. "Suprathreshold stochastic resonance and signal-to-noise ratio improvement in arrays of comparators", Physics Letters A, 321,280–290, 2004. DOI: 10.1371/journal.pone.0058507

[27] P. E. Greenwood, L. M. Ward, W. Wefelmeyer, "Statistical analysis of stochastic resonance in a simple setting" , Physical Review E, 60, 4687–4695, 1999. DOI: 10.1103/physreve.60.4687

[28] M. E. Inchiosa, J. W. C. Robinson, A. R. Bulsara, "Information-theoretic stochastic resonance in noise-floor limited systems: the case for adding noise", Physical Review Letters, 85, 3369–3372, 2000. DOI: 10.1103/PhysRevLett.85.3369

[29] M. D. McDonnell, D. Abbott, C. E. M. Pearce, "Analysis of noise enhanced information transmission in an array of comparators", Microelectronics Journal, 33, 1079–1089, 2002. DOI: 10.1016/S0026-2692(02)00113-1

[30] L. Gammaitoni, M. Locher, A. Bulsara, P. H¨anggi, J. Neff, K. Wiesenfeld, W. Ditto, M. E. Inchiosa. Controlling stochastic resonance, Physical Review Letters, 82, 4574–4577, 1999. DOI: 10.1103/PhysRevLett.82.4574

[31] G. P. Harmer, B. R. Davis, D. Abbott, "A review of stochastic resonance: circuits and measurement", IEEE Transactions on Instrumentation and Measurement, 51, 299–309, 2002. DOI: 10.1109/19.997828

[32] A. M. Safian, U. Rashid, "Optimization of Stochastic-Resonance based Schmitt trigger through parametric analysis". Third International Conference on Electrical Engineering, 2009: 1-6, 2009. DOI: 10.1109/ICEE.2009.5173183

[33] Digital potentiometer datasheet X9313, 2020. https://www.renesas.com/eu/en/products/data-converters/digital potentiometers/dcp/device/X9313.html.

[34] B.Zhou, M.D.McDonnell, Optimising threshold levels for information transmission in binary threshold networks: Independent multiplicative noise on each threshold, Physica A 419, 659–667, 2015. DOI: 10.1016/j.physleta.2015.05.032

[35] A. R. Silva, M. J. Oliveira (advisor). Stochastic resonance: general study and its application for the generation of the second harmonic. Dissertation (Physics) Physics Institute of the São Paulo University, São Paulo, 2011 (in Portuguese).